

# Myopic deconvolution of adaptive optics retina images

L. Blanco<sup>a,b</sup>, L.M. Mugnier<sup>a</sup> and M. Glanc<sup>b</sup>

<sup>a</sup>Office National d'Études et de Recherches Aérospatiales (ONERA), Optics  
Department, BP.72, F-92322 Châtillon, France;

<sup>b</sup>Observatoire de Paris-Meudon, Laboratoire d'Études Spatiales et d'Instrumentation en  
Astrophysique, 5 place Jules-Janssen, 92195 Meudon cedex, France

## ABSTRACT

Adaptive Optics corrected flood imaging of the retina is a well-developed technique. The raw images are usually of poor contrast because they are dominated by an important background, and because AO correction is only partial. Interpretation of such images is difficult without an appropriate post-processing, typically background subtraction and image deconvolution. Deconvolution is difficult because the PSF is not well-known, which calls for myopic/blind deconvolution, and because the image contains in-focus and out-of-focus information from the object. In this communication, we tackle the deconvolution problem. We model the 3D imaging by assuming that the object is approximately the same in all planes within the depth of focus. The 3D model becomes a 2D model with the global PSF being an unknown linear combination of the PSF for each plane. The problem is to estimate the coefficients of this combination and the object. We show that the traditional method of joint estimation fails even for a small number of coefficients. We derive a marginal estimation of unknown hyperparameters (PSF coefficients, object Power Spectral Density and noise level) followed by a MAP estimation of the object. Such a marginal estimation has better statistical convergence properties, and allows us to obtain an "unsupervised" estimate of the object. Results on simulated and experimental data are shown.

**Keywords:** Retinal imaging, myopic deconvolution, adaptive optics, unsupervised estimation, inverse problems

## 1. INTRODUCTION

Early detection of retina pathologies such as age related macula degeneration, glaucoma or retinitis pigmentosa, which is crucial in dealing with these conditions, calls for in vivo cellular level resolution eye fundus imaging. However, in vivo retina imaging suffers from the poor optical quality of the eye anterior segment (lens, cornea, tear film) and the movements of the eye. Adaptive optics (AO) is a well-known opto-mechanical technique for compensating for the time-varying aberrations of the eye. However, AO correction is only partial and uncorrected aberrations remain. Raw images are also dominated by an important background. Moreover, the object is three-dimensional and out-of-focus planes of the object also contribute to the image formation, resulting in a blurred image. A deconvolution step, taking into account the 3D nature of the object, is therefore necessary to restore the lateral resolution of the retina images. Deconvolution of retinal images is difficult because the point spread function (PSF) is not well-known, we must therefore jointly estimate the PSF and the object, a technique known as blind/myopic deconvolution. The 2D image is a slice of a convolution of the 3D object and the 3D PSF of our optical system. We work on simulated 2D images similar to images obtained with an AO eye fundus imager and on experimental data (image and wavefront data from a Hartmann-Shack wavefront sensor) recorded with the eye-fundus imager of the Center for Clinical Investigation of the Quinze-Vingts Hospital in Paris, developed by the Observatoire de Paris-Meudon.

---

Further author information: (Send correspondence to L.B.)

E-mail: leonardo.blanco@onera.fr, Telephone: +33(0)1 46 73 48 46

## 2. DECONVOLUTION METHODS

### 2.1 Imaging model

We model the image formation as a 3D convolution:

$$\mathbf{i} = \mathbf{h} *_3 \mathbf{o} + \mathbf{n} + \mathbf{b}, \quad (1)$$

where  $\mathbf{i}$  is the 3D image,  $\mathbf{o}$  is the 3D object,  $*_3$  denotes the 3D convolution operator,  $\mathbf{h}$  is the 3D PSF,  $\mathbf{n}$  is the noise and  $\mathbf{b}$  is the background.

$$i_{3D}(x, y, z) = \iiint o_{3D}(x - x', y - y', z - z') \cdot h_{3D}(x', y', z') dx' dy' dz' + n(x, y, z) + b(x, y, z)$$

We assume that our object, the photoreceptor mosaic, is, within the depth of focus of our instrument, shift invariant along the optical axis.

$$o_{3D}(x, y, z) = o(x, y) \cdot a(z)$$

where  $a(z)$  is the normalized flux emitted by the plane at depth  $z$  ( $\int a(z) dz = 1$ ).

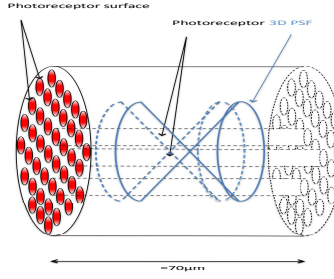


Figure 1. Photoreceptor model with 2 PSFs.

$$i_{3D}(x, y, z) = \iiint o_{3D}(x - x', y - y') \cdot a(z - z') \cdot h_{3D}(x', y', z') dx' dy' dz' + n(x, y, z)$$

In one plane ( $z = 0$ ), we have:

$$\begin{aligned} i_{3D}(x, y, z = 0) &= \iiint o(x - x', y - y') \cdot a(-z') \cdot h_{3D}(x', y, z') dx' dy' dz' + n(x, y) \\ i(x, y) \triangleq i(x, y, z = 0) &= o(x, y) *_2 \int a(-z') \cdot h_{3D}(x, y, z') dz' + n(x, y) \end{aligned} \quad (2)$$

With this model, the 2D image  $i(x, y)$  at the focal plane of the instrument is the 2D convolution of a 2D object and a global PSF  $\mathbf{h}$  which is the linear combination of the individual 2D PSFs (each one associated with a different plane of the object) weighted by the back-scattered flux at each plane ( $\mathbf{h} = \sum_j \alpha_j \mathbf{h}_j$ ). The 2D PSFs differ only by a defocus ( $\mathbf{h}_j = \mathbf{h}_0(\phi_0 + \delta\phi_j)$ , where  $\delta\phi_j$  is a pure defocus and  $\phi_0$  can be obtained from the WFS). Since data are discrete arrays and for a finite number  $N$  of planes, we have:

$$\mathbf{i} = \left( \sum_{j=0}^{N-1} a_j \mathbf{h}_j \right) * \mathbf{o} + \mathbf{n} + \mathbf{b}, \quad (3)$$

where  $\mathbf{h}_j$  is the 2D PSF at plane  $j$ . In the following, we will note  $\mathbf{a}$  the vector that contains the PSF decomposition coefficients  $a_j$ . We must estimate  $\mathbf{o}$  and  $\mathbf{a}_j$ .

## 2.2 Joint Estimation

The classical myopic deconvolution approach is to perform a joint estimation of both the object and the PSF<sup>1,2,3</sup>. Following the Bayesian approach, we compute the joint maximum *a posteriori* (jmap) estimator:

$$(\hat{\mathbf{o}}, \hat{\mathbf{a}}) = \arg \max_{\mathbf{o}, \mathbf{a}} p(\mathbf{i}, \mathbf{o}, \mathbf{a}; \theta) \quad (4)$$

$$= \arg \max_{\mathbf{o}, \mathbf{a}} p(\mathbf{i}|\mathbf{o}, \mathbf{a}; \theta) p(\mathbf{o}; \theta) \quad (5)$$

where,  $p(\mathbf{i}, \mathbf{o}, \mathbf{a}; \theta)$  is the joint probability density of the data ( $\mathbf{i}$ ), of the object ( $\mathbf{o}$ ), and of the PSF decomposition coefficients ( $\mathbf{a}$ ). It may depend on set of regularization parameters or hyperparameters ( $\theta$ ).  $p(\mathbf{i}|\mathbf{o}, \mathbf{a}; \theta)$  is the likelihood of the data  $\mathbf{i}$  and  $p(\mathbf{o}; \theta)$  is the *a priori* probability density function of the object  $\mathbf{o}$ .

$\hat{\mathbf{o}}$  and  $\hat{\mathbf{a}}$  can therefore be defined as the estimated object and coefficients that minimize a criterion  $J(\mathbf{o}, \mathbf{a})$  defined as follows:

$$J_{jmap}(\mathbf{o}, \mathbf{a}) = J_i(\mathbf{o}, \mathbf{a}) + J_o(\mathbf{o}, \mathbf{a}), \quad (6)$$

where  $J_i(\mathbf{o}, \mathbf{a}) = -\ln p(\mathbf{i}|\mathbf{o}, \mathbf{a}; \theta)$  (fidelity to the data) and  $J_o = -\ln p(\mathbf{o}; \theta)$  (regularization term). We assume that the noise is stationary white Gaussian with a variance  $\sigma^2$ . For the object, we choose a Gaussian prior probability distribution with a mean value  $\mathbf{o}_m$  and a covariance matrix  $R_o$ . The set of hyperparameters is therefore  $\theta = (\sigma^2, \mathbf{o}_m, R_o)$ . Under these assumptions, we have:

$$\begin{aligned} p(\mathbf{i}, \mathbf{o}, \mathbf{a}; \theta) &= \frac{1}{(2\pi)^{\frac{N^2}{2}} \sigma^{N^2}} \exp \left( -\frac{1}{2\sigma^2} (\mathbf{i} - H\mathbf{o})^t (\mathbf{i} - H\mathbf{o}) \right) \\ &\times \frac{1}{(2\pi)^{\frac{N^2}{2}} \det(R_o)^{1/2}} \exp \left( -\frac{1}{2} (\mathbf{o} - \mathbf{o}_m)^t R_o^{-1} (\mathbf{o} - \mathbf{o}_m) \right) \\ J_{jmap}(\mathbf{o}, \mathbf{a}) &= \frac{1}{2} N^2 \ln \sigma^2 + \frac{1}{2\sigma^2} (\mathbf{i} - H\mathbf{o})^t (\mathbf{i} - H\mathbf{o}) \\ &+ \frac{1}{2} \ln \det(R_o) + \frac{1}{2} (\mathbf{o} - \mathbf{o}_m)^t R_o^{-1} (\mathbf{o} - \mathbf{o}_m) + C, \end{aligned} \quad (7)$$

where  $H$  is the operator performing the convolution by the PSF  $\mathbf{h}$ ,  $\det(x)$  is the determinant of matrix  $x$ ,  $N^2$  is the number of pixels in the image and  $C$  is a constant. By cancelling the derivative of  $J(\mathbf{o}, \mathbf{a})$  with respect to the object, we obtain an analytical expression of the object  $\hat{\mathbf{o}}(\mathbf{a}; \theta)$  that minimizes the criterion for a given  $(\mathbf{a}; \theta)$ :

$$\hat{\mathbf{o}}(\mathbf{a}, \theta) = (H^t H + \sigma^2 R_o^{-1})^{-1} (H^t \mathbf{i} + \sigma^2 R_o^{-1} \mathbf{o}_m) \quad (8)$$

Since the matrices  $H$  (convolution operator) and  $R_o$  (covariance matrix of a Gaussian object) are Toeplitz-block-Toeplitz, we can write the joint criterion  $J_{jmap}$  and the analytical expression of the object  $\hat{\mathbf{o}}(\mathbf{a}, \theta)$  in the Fourier domain with a circulant approximation:

$$\begin{aligned} J_{jmap}(\mathbf{o}, \mathbf{a}) &= \frac{1}{2} N^2 \ln S_b + \frac{1}{2} \sum_{\nu} \frac{|\tilde{i} - \tilde{h}\tilde{o}|^2}{S_b} \\ &+ \frac{1}{2} \sum_{\nu} \ln S_o(\nu) + \frac{1}{2} \sum_{\nu} \frac{|\tilde{o}(\nu) - \tilde{o}_m(\nu)|^2}{S_o(\nu)} \end{aligned} \quad (9)$$

$$\text{and } \hat{\tilde{o}}(\nu) = \frac{\tilde{h}^*(\nu) \tilde{i}(\nu) + \frac{S_b \tilde{o}_m(\nu)}{S_o(\nu)}}{|\tilde{h}(\nu)|^2 + \frac{S_b}{S_o(\nu)}}, \quad (10)$$

where  $S_b$  is the noise power spectral density (PSD),  $S_o$  is the object PSD,  $\nu$  is the spatial frequency and  $\tilde{x}$  denotes the two-dimensional Fast Fourier Transform of  $x$ .

If we substitute Eq. (10) into (9), we obtain a new expression of  $J_{jmap}$  that does not depend explicitly on the object:

$$J'_{jmap}(\mathbf{a}) = \frac{1}{2}N^2 \ln S_b + \frac{1}{2} \sum_{\nu} \ln S_o(\nu) + \frac{1}{2} \sum_{\nu} \frac{1}{S_o(\nu)} \frac{|\tilde{i}(\nu) - \tilde{h}(\nu)\tilde{o}_m(\nu)|^2}{|\tilde{h}(\nu)|^2 + \frac{S_b}{S_o(\nu)}}. \quad (11)$$

Even if the hyperparameters  $S_b$  and  $S_o$  are known (whis is not realistic in practice), such a joint criterion does not, in general, have good asymptotic properties (citation). Moreover, we show in subsection 3.1 that the joint estimator degenerates for our problem, even in the most simple cases. This is why we propose the marginal estimator, which is known to have better statistical properties.<sup>4</sup>

### 2.3 Marginal estimation

In this method, we first estimate the PSF coefficients and the hyperparameters ( $\mathbf{a}$ ,  $S_b$ ,  $S_o$ ) before restoring the object for the estimated ( $\mathbf{a}$ ,  $S_b$ ,  $S_o$ ). The marginal estimator allows us to also estimate the noise and object hyperparameters on the image whereas, in the joint estimator case, the hyperparameters had to be empirically adjusted.

#### 2.3.1 Marginal criterion

Marginal estimation of the coefficients  $\mathbf{a}$  consists in integrating the object out of the problem (marginalizing), i.e. computing the probability law by summing over all possible values of the object. The marginal estimator is therefore a maximum likelihood estimator for the coefficients  $\mathbf{a}$ :

$$\hat{\mathbf{a}}_{ML} = \arg \max_{\mathbf{a}} \int p(\mathbf{i}, \mathbf{o}, \mathbf{a}; \theta) d\mathbf{o} \quad (12)$$

$$= \arg \max_{\mathbf{a}} p(\mathbf{i}, \mathbf{a}; \theta) = \arg \max_{\mathbf{a}} p(\mathbf{i}|\mathbf{a}; \theta)p(\mathbf{a}; \theta). \quad (13)$$

We keep the assumptions made for the joint estimation (stationary white Gaussian noise, Gaussian prior for the object). Since  $\mathbf{i}$  is a linear combination of a Gaussian object and a Gaussian noise, it is also Gaussian. Its associated probability density reads:

$$p(\mathbf{i}|\mathbf{a}; \theta) = A(\det R_i)^{-1/2} \exp \left( -\frac{1}{2}(\mathbf{i} - \mathbf{i}_m)^t R_i^{-1}(\mathbf{i} - \mathbf{i}_m) \right), \quad (14)$$

where  $A$  is a constant,  $R_i$  is the image covariance matrix and  $\mathbf{i}_m = \langle \mathbf{i} \rangle$ .

Maximizing  $p(\mathbf{i}|\mathbf{a}; \theta)$  is equivalent to minimizing the opposite of its logarithm:

$$J_{ML}(\mathbf{a}) = \frac{1}{2} \ln \det(R_i) + \frac{1}{2}(\mathbf{i} - \mathbf{i}_m)^t R_i^{-1}(\mathbf{i} - \mathbf{i}_m) + B \quad (15)$$

where  $B$  is a constant and  $R_i = HR_oH^t + \sigma^2 I_d$  ( $I_d$  is the identity matrix). The marginal criterion can be written in the Fourier domain as follows:

$$J_{ML}(\mathbf{a}) = \frac{1}{2} \sum_{\nu} \ln S_o(\nu) + \frac{1}{2} \sum_{\nu} \ln \left( |\tilde{h}(\nu)|^2 + \frac{S_b}{S_o(\nu)} \right) + \frac{1}{2} \sum_{\nu} \frac{1}{S_o(\nu)} \frac{|\tilde{i}(\nu) - \tilde{h}(\nu)\tilde{o}_m(\nu)|^2}{|\tilde{h}(\nu)|^2 + \frac{S_b}{S_o(\nu)}} + A'. \quad (16)$$

### 2.3.2 Hyperparameters estimation

The marginal estimator allows us to estimate the set of hyperparameters  $\theta$  (actually the object PSD  $S_o$  and noise PSD  $S_n$ ) together with the PSF coefficients in an automatic manner. This is called unsupervised estimation:

$$(\hat{\mathbf{a}}, \hat{\theta}) = \arg \max_{\mathbf{a}, \theta} f(\mathbf{i}, \mathbf{a}, \theta). \quad (17)$$

The object PSD  $S_o$  is modeled, in the Fourier domain, in the following way:<sup>5</sup>

$$S_o(\nu) = \frac{k}{1 + \left(\frac{\nu}{\nu_0}\right)^p} \quad (18)$$

and, since the noise is assumed to be Gaussian and homogeneous,  $S_b = \text{constant}$ . The criterion  $J_{ML}(\mathbf{a})$  becomes  $J_{ML}(\mathbf{a}, S_b, k, \nu_0, p)$  and must now be minimized versus the PSF coefficients  $\mathbf{a}$  and the hyperparameters  $S_b, k, \nu_0$  and  $p$ . With the change of variable  $\mu = S_b/k$ , if we cancel the derivative of the criterion with respect to  $k$ , we obtain an analytical expression  $\hat{k}(\mathbf{a}, \mu, \nu_0, p)$  that minimizes the criterion for a given value of the other parameters.  $\hat{\mu}$ ,  $\hat{\nu}_0$  and  $\hat{p}$  are then numerically estimated with a gradient-based method (Variable Metric with Limited Memory (VMLM)).

## 3. RESULTS

### 3.1 Joint estimation

A simple simulation was performed to evaluate the performance of the joint estimator in our problem. The global PSF used in the simulation is the sum of only two PSF's, the first one being focused and the second one defocused:

$$\mathbf{i} = (\alpha * \mathbf{h}_{foc} + (1 - \alpha)\mathbf{h}_{defoc}) * \mathbf{o} + \mathbf{n}, \quad (19)$$

where  $\mathbf{i}$  is the simulated image,  $\alpha$  is the PSF decomposition coefficient (in this simulation,  $\alpha = 0.3$ ),  $\mathbf{h}_{defoc}$  is the simulated defocused PSF,  $\mathbf{h}_{foc}$  is the simulated focused PSF,  $\mathbf{o}$  is the simulated object and  $\mathbf{n}$  is the noise. The object used in this simulation is a resampled version of an experimental image from the Quinze-Vingts Hospital retinal imager.

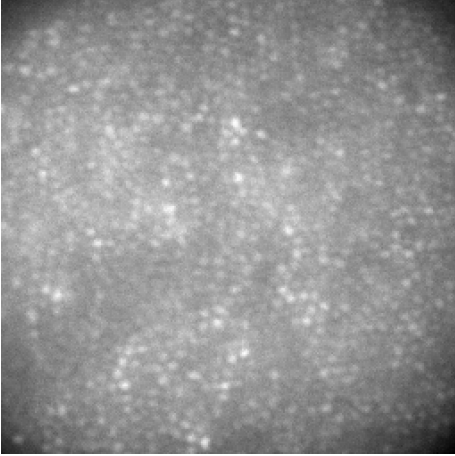


Figure 2. Simulated object

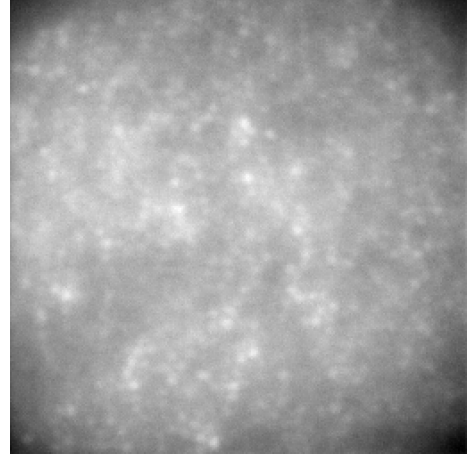


Figure 3. Simulated image

We can compute the joint criterion  $J_{jmap}(\alpha; S_o, S_b)$  (Eq. 11) for values of  $\alpha$  between 0 and 1 to find the value of alpha that minimizes the joint criterion (the object and noise PSDs are known). Figure 4 shows the result of such a computation and figure 5 the restored object for the value of  $\alpha$  that minimizes  $J_{jmap}(\alpha; S_o, S_b)$  :

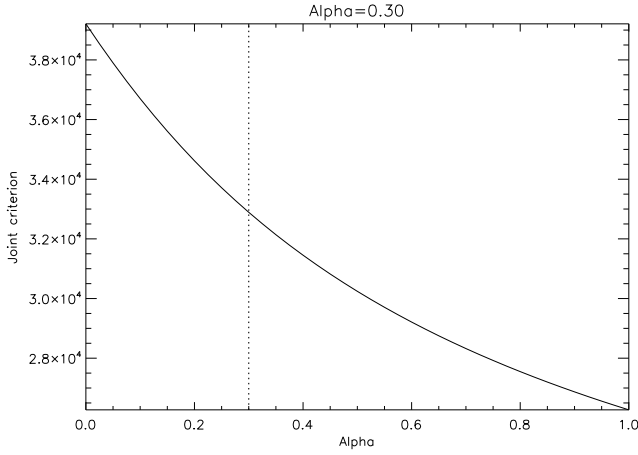


Figure 4. Joint criterion for  $0 \leq \alpha \leq 1$

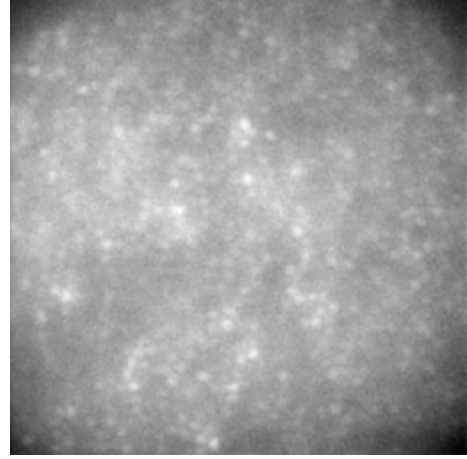


Figure 5. Joint estimated object

Figure 4 shows us that the joint estimator is minimum for  $\alpha = 1$  whereas the real value of  $\alpha$  is 0.3. The joint estimation fails to retrieve the actual value even in this very simple case (two point spread functions, known hyperparameters). The joint estimator degenerates in the case of myopic deconvolution of retinal images.

### 3.1.1 Marginal estimation

We now present the results of the marginal estimation on simulated data, first in the supervised case (known hyperparameters) and then in the unsupervised case (unknown hyperparameters).

**Supervised marginal estimation** The same simulation as in the joint estimation was performed. The marginal criterion of Eq(16) was computed for  $0 \leq \alpha \leq 1$ , also with known hyperparameters. The object is restored by Wiener filtering. The results of the computation are shown on figure 6 and the restored object on figure 7.

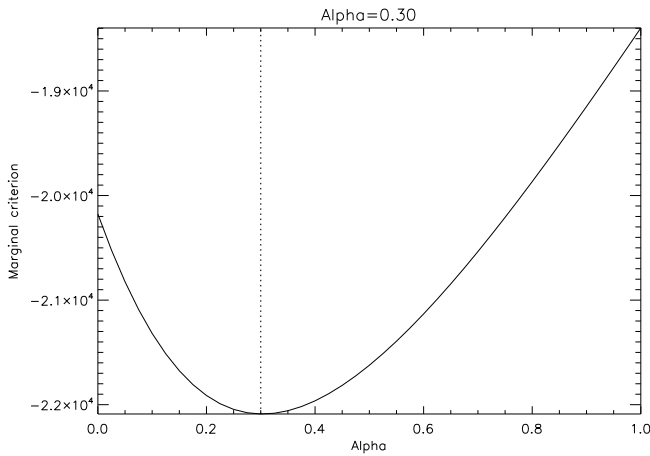


Figure 6. Marginal criterion for  $0 \leq \alpha \leq 1$

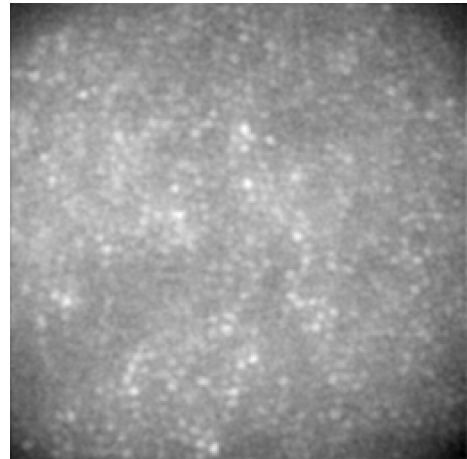


Figure 7. Marginal estimated object

The marginal criterion is minimum for  $\alpha = 0.3$ , which is the true value of  $\alpha$  used in the simulation. Figure 6 shows that the marginal estimator allows for myopic deconvolution of retinal images with our image model. Let's see its behaviour in the more realistic case of unsupervised estimation, i.e. with unknown hyperparameters.

**Unsupervised marginal estimation** In the unsupervised marginal estimation, we estimate the hyperparameters and the PSF coefficients at the same time. We have checked by simulation (same simulation conditions as in the joint and supervised marginal estimation) that the marginal estimator converges asymptotically towards the true parameters. Figure (8) shows the RMS error on the PSF coefficient estimation for different values of noise and a varying data size. We show that the marginal estimator RMS error tends towards zero when

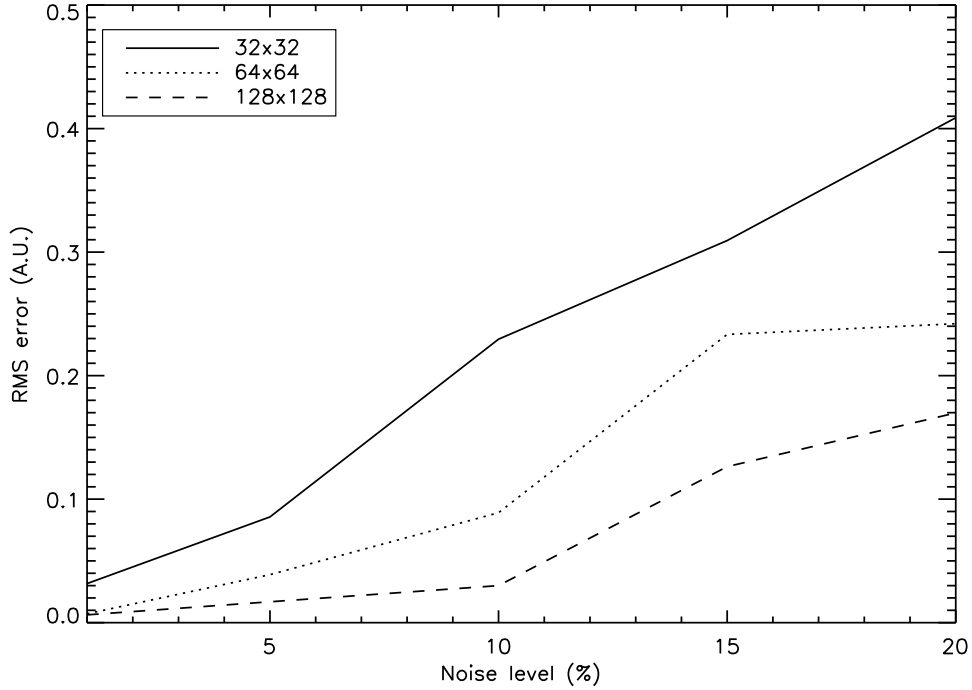


Figure 8. RMSE of PSF coefficient estimation as a function of noise level in percent (ratio between noise standard deviation and image maximum). The solid, dotted and dashed lines correspond, respectively, to images of dimensions  $32 \times 32$ ,  $64 \times 64$  and  $128 \times 128$  pixels.

noise decreases and also diminishes when the size of data increases. In particular, for an  $256 \times 256$  pixel image and noise RMS= 5%, the RMS error on the PSF coefficient  $\alpha$  estimation is less than 0.3%. The unsupervised marginal estimator is therefore consistent which opens the way to its use on experimental images.

### 3.2 Preliminary experimental results

We are now showing experimental results of the marginal estimation of the PSF on experimental data. The data are  $256 \times 256$  pixel images recorded with the Adaptive Optics eye-fundus imager of the Center for Clinical Investigation of the Quinze-Vingts Hospital in Paris, developed by the Observatoire de Paris-Meudon. No wavefront data was recorded so we assume that the adaptive optics has perfectly corrected the wavefront and that the focused PSF is a perfect Airy disk. We model the global PSF as a linear combination of 3 PSFs, the first one being focused, the second one being defocused with a focus of  $\pi/2$  rad RMS and the third one being defocused by  $\pi$  rad RMS :

$$h(x, y) = \alpha_0 h_0(x, y; \phi = 0) + \alpha_1 h_1(x, y; \phi = 0) + \alpha_2 h_2(x, y).$$

We must estimate  $\alpha = \alpha_1, \alpha_2, \alpha_3$ . The unsupervised marginal estimation gives  $\alpha = 0.41, 0.00, 0.59$ . For this image, the global estimated PSF is therefore the combination of only the most focused PSF and the less focused one. Figure (9) shows the experimental image and Fig (10) the restored object after unsupervised marginal estimation.

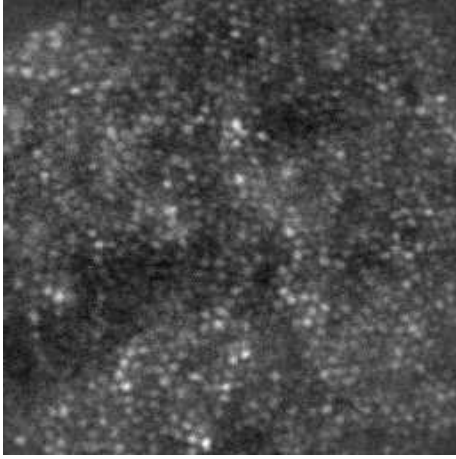


Figure 9. Experimental image

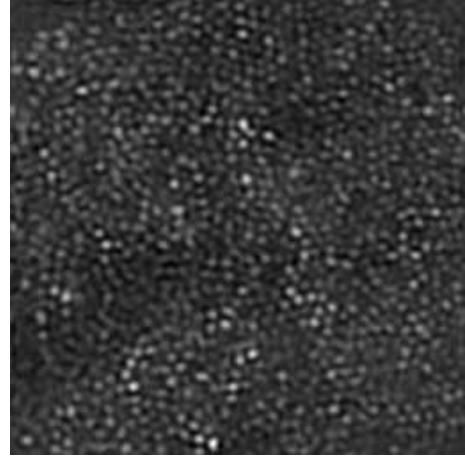


Figure 10. Restored object

It is clearly visible that the restored object is much sharper than the original image. The photoreceptors have a much better contrast and can be seen clearly throughout the image. The restored object also is much less noisy than the original image.

These preliminary results show that our image model and the marginal estimator are well adapted to the deconvolution of adaptive optics corrected retinal images.

#### 4. DISCUSSION

We have demonstrated that the classical blind joint estimation fails to retrieve the PSF, even in very simple cases. The joint estimator is degenerated in the case of blind deconvolution of adaptive optics. We have presented a marginal estimator and showed on simulations that it was capable of restoring the PSF accurately both in the supervised and unsupervised cases. The good statistical properties of the unsupervised marginal estimation have been demonstrated (the estimates converge towards the true value as the data tends towards infinity or noise tends towards zero), making it a good candidate for experimental data myopic deconvolution. Finally, we have shown a preliminary result on real data, showing the efficiency of the marginal estimator for myopic deconvolution of adaptive optics retinal images.

#### REFERENCES

1. G. R. Ayers and J. C. Dainty, "Iterative blind deconvolution and its applications," *Opt. Lett.* **13**, pp. 547–549, 1988.
2. J. C. Christou, A. Roorda, and D. R. Williams, "Deconvolution of adaptive optics retinal images," *J. Opt. Soc. Am. A* **21**, pp. 1393–1401, Aug 2004.
3. L. M. Mugnier, T. Fusco, and J.-M. Conan, "Mistral: a myopic edge-preserving image restoration method, with application to astronomical adaptive-optics-corrected long-exposure images," *J. Opt. Soc. Am. A* **21**, pp. 1841–1854, Oct 2004.
4. A. Blanc, L. M. Mugnier, and J. Idier, "Marginal estimation of aberrations and image restoration by use of phase diversity," *J. Opt. Soc. Am. A* **20**, pp. 1035–1045, Jun 2003.
5. J.-M. Conan, L. M. Mugnier, T. Fusco, V. Michau, and G. Rousset, "Myopic deconvolution of adaptive optics images by use of object and point-spread function power spectra," *Appl. Opt.* **37**, pp. 4614–4622, Jul 1998.